44th Annual Symposium of the Ultrasonic Industry Association, UIA 44th Symposium, 20-22 April 2015, Washington, DC, USA and of the 45th Annual Symposium of the Ultrasonic Industry Association, UIA 45th Symposium, 4-6 April 2016, Seattle, WA, USA

Development of an Ultrasonic Resonator for Ballast Water Disinfection

Hafiiz Osman[a,b]*, Fannon Lim[b], Margaret Lucas[b], Prakash Balasubramaniam[a]

[a]*Sembcorp Marine Ltd., 29 Tanjong Kling Road, S628054, Singapore*
[b]*School of Engineering, University of Glasgow, Glasgow, G12 8QQ, UK*

Abstract

Ultrasonic disinfection involves the application of low-frequency acoustic energy in a water body to induce cavitation. The implosion of cavitation bubbles generates high speed microjets >1 km/s, intense shock wave >1 GPa, localized hot spots >1000 K, and free-radicals, resulting in cell rupture and death of micro-organisms and pathogens. Treatment of marine ballast water using power ultrasonics is an energy-intensive process. Compared with other physical treatment methods such as ultraviolet disinfection, ultrasonic disinfection require 2 to 3 orders of magnitude more energy to achieve similar rate of micro-organism mortality. Current technology limits the amount of acoustic energy that can be transferred per unit volume of fluid and presents challenges when it comes to high-flow applications. Significant advancements in ultrasonic processing technology are needed before ultrasound can be recognized as a viable alternative disinfection method. The ultrasonic resonator has been identified as one of the areas of improvement that can potentially contribute to the overall performance of an ultrasonic disinfection system. The present study focuses on the design of multiple-orifice resonators (MOR) for generating a well-distributed cavitation field. Results show that the MOR resonator offers significantly larger vibrational surface area to mass ratio. In addition, acoustic pressure measurements indicate that the MOR resonators are able to distribute the acoustic energy across a larger surface area, while generating 2-4 times higher pressures than existing ultrasonic probes.

---

* Corresponding author. Tel.: +65-9680-9571.
  E-mail address: hafiiz.osman@sembmarine.com

1. Introduction

Ultrasonic cavitation has very limited application in large-scale treatment plants due to the inherent limitations of ultrasonic devices (Gavand et al. 2007; Hunter et al. 2008). Collings et al (2007) and Stamper et al. (2008) have demonstrated the use of ultrasound in ballast water treatment and found it to be effective, but would require prohibitively high power consumption if implemented as a full-scale shipboard system. A review of literature revealed that most studies in this area utilize standard off-the-shelf ultrasonic probe devices that are not intended for the large-scale, high flow applications. An inherent limitation of these devices is the concentration of high intensity acoustic energy over a small surface area, generating a cavitation region that is confined to a very small volume near the tip of the probe device. To overcome this limitation, the use of multiple probe-type devices has been proposed (Gogate et al. 2011). There have also been efforts to increase the cavitation region through novel horn design such as those investigated by Wei et al. (2015) and Xu et al. (2011). The present study describes the development of the MOR resonator which has a large radiating surface area to mass ratio with the aim of generating a strong and well-distributed cavitation field.

2. Design of MOR resonators

The MOR resonator consists of mechanically-coupled L-section and R-section as shown in Fig. 1a. The L-section is designed to operate in the first longitudinal mode (L1) while the R-section is designed to operate in the fundamental radial mode (R0) at the operating frequency. In designing the MOR resonators, the L and R sections are designed and analyzed separately. Once the design of the two sections is satisfactory, they are assembled to form the MOR resonator and further analysis is carried out. Although the L and R sections are individually tuned to the L1 and R0 mode at the operation frequency, the MOR resonator assembly requires further analysis to identify the shifts in resonance frequencies and the possible excitation of parasitic modes resulting from the coupling. The resonance frequency shift can be compensated by further tuning while parasitic modes may be minimized or eliminated through various design strategies (Cardoni et al. 2003; Mathieson & Lucas 2015).
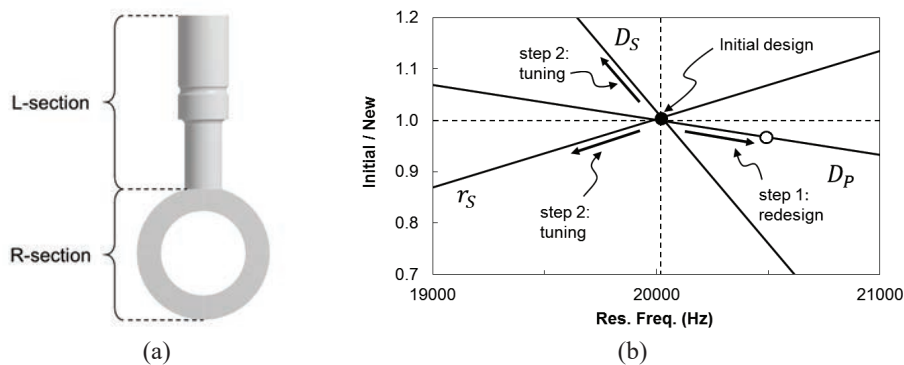

Fig. 1. (a) MOR resonator with P-type R-section; (b) MOR resonator tuning chart.

The R-section design was determined iteratively through finite element method. R-section outer diameter and axial length were kept constant, and specific parameters related to the orifice dimensions and positions were varied. Various R-section designs are possible and the designs can be broadly classified as P-type, PS-type, and PST-type depending on the orifice configuration. For the sake of brevity, a P-type design has only the primary orifice; the PS-type design is identified by the presence of a secondary layer of orifices; and the PST-type design has in addition a tertiary layer of orifices. In Fig. 1b, derivation of variant PST horn designs is succinctly illustrated. The procedure begins with the assumption that a particular tuned P, PS, or PST configuration exists. From this initial design, one of the geometric design parameter is adjusted (in this example, the primary orifice diameter D_p) and the device is subsequently tuned by adjusting the other design parameters (secondary orifice diameter D_s and radial position r_s).

A commercial finite element code (ANSYS 15.0) was used to carry out computations for free vibration analysis enabling the extraction of mode shapes and corresponding modal frequencies for each design. Dynamic response of the structure was then modeled by applying an excitation force at the input face of the L-section to simulate the vibrational input from an external exciter. Frequency response (FRF) of the designs was then extracted and the excited modes in the frequency range of interest was identified. It is to be noted that the finite element design at this stage do not involve computational fluid dynamics and the effect of water loading is not being considered. A global damping ratio of 0.3% was applied for all cases. A hexahedral meshing scheme was used where feasible, otherwise a dense tetrahedral mesh was implemented to obtain accurate results. Mesh sensitivity analysis was carried out to determine the appropriate mesh density, with results showing that mesh convergence was achieved with approximately 20,000 elements.

3. Evaluation of LR resonators

3.1. Radiating surface area

Based on the methodology outlined in Section 2, three PS-type radial resonator designs were derived. Each design was coupled to the same L-section to produce the LPS-type resonator as shown in Table 1. The LP-type resonator, formed through the coupling of an L-section with a single-orifice R-section (i.e. P-type), is included for comparison. Coupling of the L and R sections appeared to have increased the L1-R0 mode resonance frequency by up to 0.6%, despite the sections being tuned to 20 kHz individually. As shown in Table 1, the shift in the L1-R0 mode frequency is influenced by the number of secondary orifices and vibration uniformity. The LPS2 design, having the least number of secondary orifices and therefore the least uniform radial displacement, exhibits greater deviation from the intended operating frequency. In terms of the objective to increase radiating surface area without increasing the mass of the device, it is apparent that the LPS-type design achieves this objective successfully, with the LPS designs offering between 75% to 100% increase in the radiating surface area on a per unit mass basis.

Table 1. Comparison of MOR resonator design outcomes

Parameters	Designs			
	LP1	LPS1	LPS2	LPS3
Mode shape				
Res. freq. (Hz)	20070	20091	20112	20097
Δ Res. freq (Hz)	+70	+73	+113	+92
Norm. mass	1.000	0.971	0.997	0.992
Norm. radiating area	1.000	1.959	1.745	1.841
Norm. area/mass	1.000	2.018	1.750	1.856

3.2. Harmonic response simulation

Responses of the devices from a forced input excitation normalized to the input amplitude are shown in Fig. 2. Comparing the 4 designs, probability of modal coupling is highest for LPS2 and LPS3 due to the presence of several

parasitic modes within 2000 Hz of the operating modes. These are attributed to complex modes resulting from the secondary orifices displacement and bending modes of the L-section. Interestingly, LPS1 does not exhibit any of said characteristics of the other two LPS-type devices. Instead, its frequency response is closer to the LP1 design and has a lower risk of modal coupling.
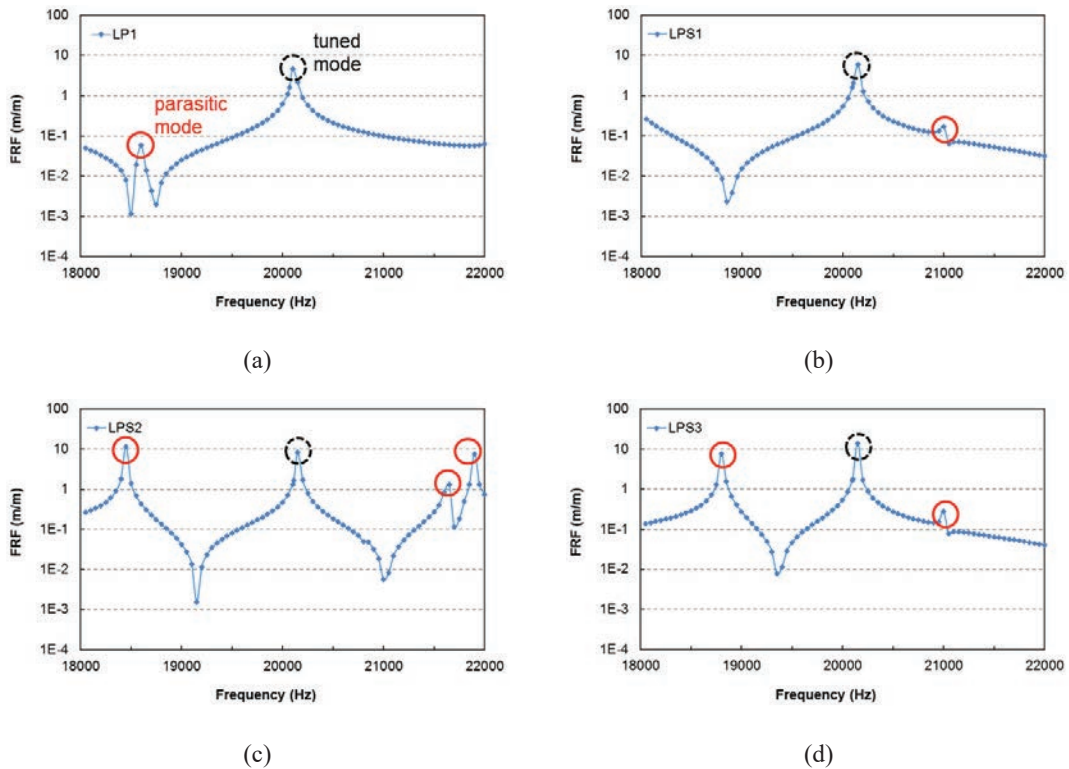

(a)

(b)

(c)

(d)

Fig. 2. Simulated FRFs for MOR resonator designs: (a) LP1; (b) LPS1; (c) LPS2; (c) LPS3.

3.3. Comparison of ultrasound-induced acoustic pressure

Following the harmonic response analysis, the LP1 and LPS1 resonators were selected for fabrication. Both devices were fabricated from aluminum with the L-section and R-section machined separately. The two sections were assembled to form the MOR resonator by means of a set screw fastener. The MOR resonator assembly was then attached to a commercial half-wave Langevin transducer tuned at 20 kHz using the same method. An electronic driver supplied the voltage waveform for exciting the transducer, providing the means to vibrate the MOR resonator at its resonance frequency.

Acoustic pressure was measured using a miniature hydrophone (TC4038, Reson, Denmark) positioned some distance from the radiating surface (A), at the geometric center of the primary orifice (B), and at the geometric center of a secondary orifice (C). Position A was selected such that a valid comparison can be made between the MOR resonator and a commercial ultrasonic probe.

Hydrophone measurements showed that for both LP1 and LPS1 resonators, peak pressure is higher at position B than at position A due to the acoustic pressure concentrating effect of the R0 mode. This is consistent with Hunter et al. (2008) observations. As shown in Fig. 3, peak pressure at position C is approximately two times higher than peak pressure at position B due to the simultaneous translation and deformation of the secondary orifices. Interestingly, while the peak pressure in the primary and secondary orifices is several orders of magnitude higher than external

peak pressure, the addition of secondary orifices seems to result in greater distribution of acoustic energy such that the peak pressure at the primary orifice is reduced by half. This is not necessarily undesirable since the pressures can be adjusted to the required level by controlling the input excitation.

Acoustic pressure from a commercial ultrasonic probe (306-02, Sonics and Materials, USA) was also measured to compare with the acoustic performance of the fabricated resonator prototypes (see Fig. 4a). As shown in Fig. 4b, LP1 and LPS1 resonators respectively generated 28% and 77% higher pressure than the commercial device when measured at position A. Pressure in the primary and secondary orifices is therefore at least 200% to 400% higher, which is a significant improvement.
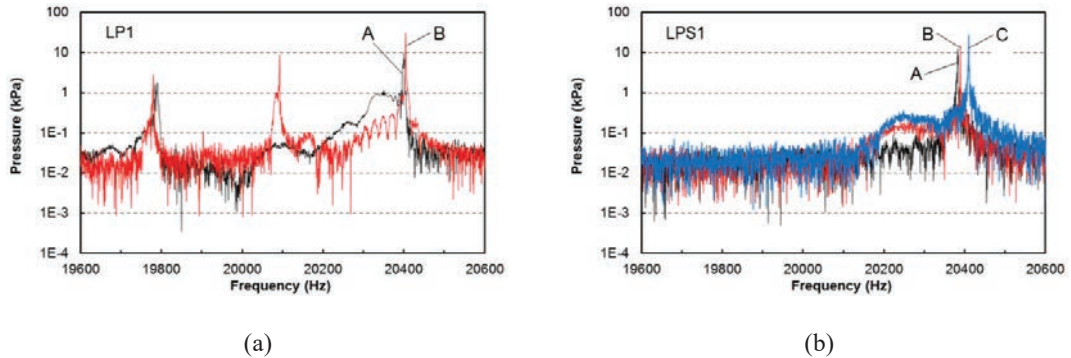

(a)　　　　　　　　　　　　　　　　　(b)

Fig. 3. Measured acoustic pressure from devices (a) LP1 and (b) LPS1; data from various hydrophone positions: A – some distance from external circumference or probe tip; B – geometric center of primary orifice; and C – geometric center of secondary orifice
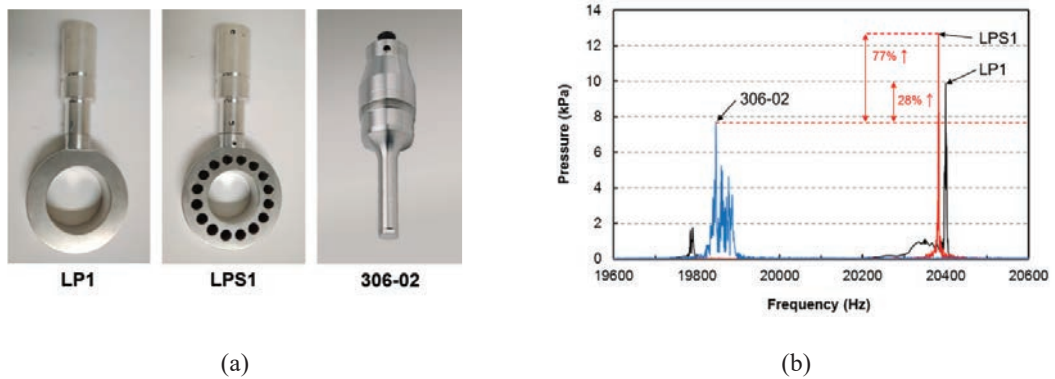

(a)　　　　　　　　　　　　　　　　　(b)

Fig. 4. (a) Fabricated devices for acoustic pressure measurement; (b) Measured acoustic pressure spectrum at position A.

4. Conclusions

This research has demonstrated that the MOR resonators can be efficiently designed by analyzing the mode shapes of the L-section and R-section separately, followed by dynamic response analysis of the MOR resonator assembly to predict modal excitation and eliminate parasitic modes through systematic design iterations. It was demonstrated that the incorporation of multiple orifices results in a two-fold increase in the radiating surface area without increasing the structural mass of the device. Fabricated MOR resonators were shown to generate significantly higher pressures when compared with commercial probe-type devices and can potentially increase

efficacy and efficiency of ultrasonic disinfection. Future work will focus on further design optimization, vibroacoustic characterization, and evaluation of the devices' biological efficacy.

Acknowledgements

References

Cardoni, A. et al., 2003. Controlling the effects of modal interactions in ultrasonic cutting devices. In *5th World Congress on Ultrasonics*. Paris, France, 7-10 September 2003, pp. 49–56.

Collings, A.F. et al., 2007. Treatment of Ballast Water By High Power Ultrasonics. *Proceedings of the 19th International Congress on Acoustics, Revista de Acustica*, 38(3-4).

Gavand, M.R. et al., 2007. Effects of sonication and advanced chemical oxidants on the unicellular green alga Dunaliella tertiolecta and cysts, larvae and adults of the brine shrimp Artemia salina: A prospective treatment to eradicate invasive organisms from ballast water. *Marine Pollution Bulletin*, 54(11), pp.1777–1788.

Gogate, P.R., Sutkar, V.S. & Pandit, A.B., 2011. Sonochemical reactors: Important design and scale up considerations with a special emphasis on heterogeneous systems. *Chemical Engineering Journal*, 166(3), pp.1066–1082. Available at: http://dx.doi.org/10.1016/j.cej.2010.11.069.

Hunter, G. et al., 2008. A radial mode ultrasonic horn for the inactivation of Escherichia coli K12. *Ultrasonics Sonochemistry*, 15(2), pp.101–109.

Mathieson, A. & Lucas, M., 2015. Minimizing the Excitation of Parasitic Modes of Vibration in Slender Power Ultrasonic Devices. *Physics Procedia*, 63, pp.42–46. Available at: http://www.sciencedirect.com/science/article/pii/S1875389215000784 [Accessed April 18, 2016].

Stamper, D.M., Holm, E.R. & Brizzolara, R.A., 2008. Exposure times and energy densities for ultrasonic disinfection of Escherichia coli, Pseudomonas aeruginosa, Enterococcus avium, and sewage. *Journal of Environmental Engineering and Science*, 7(2), pp.139–146.

Wei, Z. et al., 2015. Designing and characterizing a multi-stepped ultrasonic horn for enhanced sonochemical performance. *Ultrasonics Sonochemistry*, 27, pp.325–333. Available at: http://linkinghub.elsevier.com/retrieve/pii/S135041771500142X.

Xu, L., Lin, S. & Hu, W., 2011. Optimization design of high power ultrasonic circular ring radiator in coupled vibration. *Ultrasonics*, 51(7), pp.815–823.